Original Article

Cone-beam computed tomography-guided shape-sensing robotic bronchoscopy *vs.* electromagnetic navigation bronchoscopy for pulmonary nodules

Ramsy Abdelghani[1]^, Diana Espinoza[1], Juan P. Uribe[2], David Becnel[1,3], Rachel Herr[1], Regina Villalobos[4], Fayez Kheir[4]

[1]Division of Pulmonary Diseases, Critical Care, and Environmental Medicine, Tulane University Medical Center, Tulane University School of Medicine, New Orleans, LA, USA; [2]Department of Internal Medicine, University of Miami, Miami, FL, USA; [3]Department of Pulmonary and Critical Care Medicine, Southeast Veterans Health Care System, New Orleans, LA, USA; [4]Division of Pulmonary and Critical Care Medicine, Massachusetts General Hospital, Harvard Medical School, Boston, MA, USA

Contributions: (I) Conception and design: R Abdelghani, F Kheir; (II) Administrative support: F Kheir; (III) Provision of study materials or patients: R Abdelghani, D Becnel; (IV) Collection and assembly of data: D Espinoza, JP Uribe, R Herr; (V) Data analysis and interpretation: JP Uribe, R Villalobos; (VI) Manuscript writing: All authors; (VII) Final approval of manuscript: All authors.

Correspondence to: Ramsy Abdelghani, MD. Division of Pulmonary Diseases, Critical Care, and Environmental Medicine, Tulane University Medical Center, Tulane University School of Medicine, 1430 Tulane Avenue, New Orleans, LA 70112, USA. Email: Rabdelgh@Tulane.edu.

Background: Electromagnetic navigation bronchoscopy (ENB) and shape-sensing robotic-assisted bronchoscopy (ssRAB) are minimally invasive technologies for the diagnosis of pulmonary nodules. Cone-beam computed tomography (CBCT) has shown to increase diagnostic yield by allowing real-time confirmation of position of lesion and biopsy tool. There is a lack of comparative studies of such platforms using CBCT guidance to overcome computed tomography to body divergence. The aim of this study was to compare the diagnostic yield of ENB- and ssRAB-guided CBCT for biopsy of pulmonary nodules.

Methods: We conducted a retrospective comparative study of consecutive patients undergoing ENB-CBCT and ssRAB-CBCT. Navigational success was defined as biopsy tool within lesion confirmed during CBCT. Diagnostic yield was assessed using two methods: (I) presence of malignancy or benign histological findings that lead to a specific diagnosis at the time of bronchoscopy, and (II) longitudinal follow-up of patients with nonspecific benign finding during bronchoscopy.

Results: ENB-CBCT was used to biopsy 97 nodules and ssRAB-CBCT was used to biopsy 111 nodules. Median size of the lesion for the ENB-CBCT group was 16.5 mm [interquartile range (IQR), 12–22 mm] as compared to 12 mm (IQR, 9–16 mm) in the ssRAB-CBCT group (P<0.001). Navigational success was 70.1% in ENB-CBCT arm as compared to 83% in ssRAB-CBCT arm respectively (P=0.03). Diagnostic yield was 66% for ENB-CBCT and 89.2% for ssRAB-CBCT (P<0.001) following bronchoscopy; 79.4% for ENB-CBCT and 95.4% for ssRAB-CBCT (P<0.001) with longitudinal follow-up data respectively. Following multivariate regression analysis adjusting for the size of the lesion, distance from the pleura, presence of bronchus sign, number of CBCT spins, and number of nodules, the odds ratio for the diagnostic yield was 4.72 [95% confidence interval (CI): 2.05–10.85; P<0.001] in the ssRAB-CBCT group as compared with ENB-CBCT. The overall rate of adverse events was similar in both groups (P=0.77).

Conclusions: ssRAB-CBCT showed increased navigational success and diagnostic yield as compared to ENB-CBCT for pulmonary nodule biopsies.

Keywords: Bronchoscopy; lung cancer; pulmonary nodule; cone-beam computed tomography (CBCT)

Submitted Feb 21, 2024. Accepted for publication Jul 05, 2024. Published online Aug 28, 2024.
doi: 10.21037/jtd-24-178
View this article at: https://dx.doi.org/10.21037/jtd-24-178

^ ORCID: 0000-0002-0048-1129.

Introduction

Lung cancer is the leading cause of cancer related deaths in the United States, with an estimated 1.5 million new lung nodules detected each year (1). Early lung cancer diagnosis has been shown to improve quality of life and 5-year survival (2). However, establishing a tissue diagnosis is important in the diagnosis and treatment of intermediate risk nodules. Furthermore, the increased use of computed tomography (CT) and adoption of lung cancer screening programs have further increased the demand for improved bronchoscopic navigation and the importance of obtaining an accurate diagnosis.

Traditionally, transbronchial biopsy using conventional flexible bronchoscopy and fluoroscopy was used to navigate to and sample pulmonary nodules with a suboptimal diagnostic yield (3). To improve upon this low yield, there have been multiple recent advancements in pulmonary nodule guidance. Electromagnetic navigation bronchoscopy (ENB) aimed at optimizing navigation success demonstrated a diagnostic yield approaching 71% in a recent meta-analysis (4). More recently, shape-sensing robotic-assisted bronchoscopy (ssRAB) has been proposed to further optimize navigational accuracy, positioning, and tissue sampling due to improved airway segmentation and stability of an articulating catheter (5-7).

Highlight box

Key findings

- Our study showed that shape-sensing robotic-assisted bronchoscopy with cone-beam computed tomography (ssRAB-CBCT) imaging had a significantly increased diagnostic yield compared to electromagnetic navigation bronchoscopy with CBCT (ENB-CBCT) imaging, which improves the current standard of care when undergoing pulmonary nodule biopsy.

What is known and what is new?

- ENB and ssRAB are minimally invasive technologies for the diagnosis of pulmonary nodules. CBCT has shown to increase diagnostic yield by allowing real-time confirmation of position of lesion and biopsy tool.
- There is a lack of comparative studies of such platforms using CBCT guidance to overcome computed tomography to body divergence. The aim of this study was to compare the diagnostic yield of ENB- and ssRAB-guided CBCT for biopsy of pulmonary nodules.

What is the implication, and what should change now?

- ssRAB-CBCT showed increased navigational success and diagnostic yield as compared to ENB-CBCT for pulmonary nodule biopsies.

Despite such improvements in navigational success and diagnostic yield, there can be discrepancies between nodule location on the preprocedural CT and during the procedure in a dynamic, breathing lung. This is termed CT-to-body divergence. Cone-beam computed tomography (CBCT) can be used during navigational bronchoscopy to provide precise position confirmation of the biopsy tool in relation to lung nodules and has been shown to improve tool in lesion confirmation, likely due to the minimization of CT-to-body divergence (4,8).

Given the development of multiple navigational platforms and their increased combined use with CBCT in the last decade, it is important to assess if diagnostic yield for pulmonary nodule evaluation has improved. To our knowledge, no studies have compared the two commonly used platforms ENB and ssRAB when both are guided by CBCT.

The aim of our study is to compare the diagnostic yield of both navigational bronchoscopic platforms using CBCT guidance. We present this article in accordance with the STROBE reporting checklist (available at https://jtd.amegroups.com/article/view/10.21037/jtd-24-178/rc).

Methods

We performed a retrospective comparative study of consecutive patients undergoing navigational bronchoscopies using ENB-CBCT and ssRAB-CBCT at a single medical center (Tulane University Medical Center, New Orleans, LA, USA) from July 2020 until May 2023. The study was conducted in accordance with the Declaration of Helsinki (as revised in 2013). This study was approved by Tulane University School of Medicine Institutional Review Board (No. 2023-128) and informed consent for this retrospective analysis was waived.

One hundred and eighty-five consecutive patients with pulmonary nodules were included in the study and assigned to 2 groups to assess the diagnostic yield based on the type of procedure: ENB-CBCT or ssRAB-CBCT. ENB-CBCT was used exclusively from July 2020 until May 2022 as it was the only navigational platform at our institution. Subsequently, ssRAB-CBCT was introduced in June 2022 and was used exclusively starting in June 2022. All the interventions were part of the standard of care for the disease, and consent was waived due to the retrospective nature of the study.

Operative technique

At our institution, board-certified interventional pulmonologists

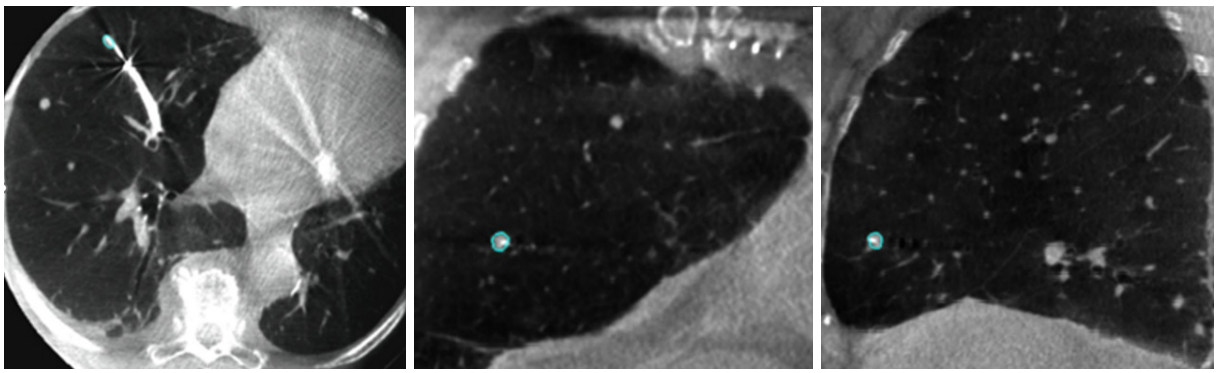

Figure 1 Cone-beam computed tomography images in axial, coronal and sagittal views of a 5 mm × 3 mm nodule with needle in lesion confirmation.

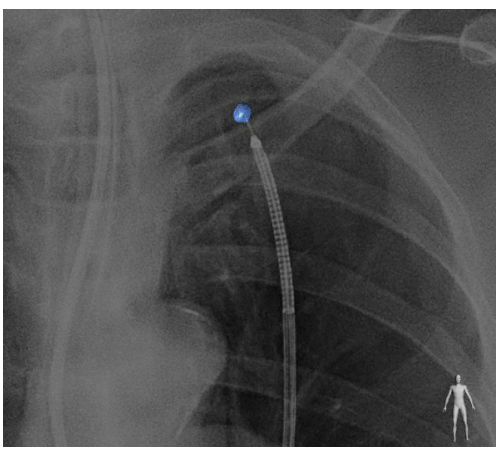

Figure 2 Augmented fluoroscopy during cone-beam computed tomography showing needle biopsy in lesion.

performed these procedures and have extensive experience with CBCT preceding this study. ENB had been used for 3 years preceding the time frame of this study. All procedures were performed under general anesthesia in a hybrid operating room equipped with a C-arm system with CBCT capabilities. All patients underwent total intravenous anesthesia, neuromuscular paralysis, and mechanical ventilation with volume control [endotracheal tube size 8.5 to 9, tidal volume of 8 cc per kilogram of ideal body weight, positive end-expiratory pressure (PEEP) between 12–16 cmH_2O as tolerated, and decreased FiO_2 as tolerated]. Continuous telemetry, pulse oximetry, and capnography were used per standard protocol for monitoring patient status during the entire procedure. Following intubation, a bronchoscope (BF-1T180; Olympus, Tokyo, Japan) was introduced to examine airways and clean secretions.

CBCT was used in all ENB and ssRAB procedures similarly. Prior to navigating to the nodule, time was taken to isocenter the patient with CBCT (Philips Allura Biplane with Lung Suite software; Philips, The Netherlands). Once navigational success was suspected, a biopsy tool was inserted followed by an 8-second CBCT spin, performed under breath-hold with adjustable pressure-limiting valve set at 20 cmH_2O, to decrease the degree of respiratory motion and atelectasis during the spin. Airway segmentation for the target lesion in multiple orthogonal planes (*Figure 1*) was done and superimposed on live fluoroscopy using dedicated software (Philips Lung Suite software). Based on tool tip location, catheter adjustments were performed under live fluoroscopy as needed. Augmented fluoroscopy is shown in *Figure 2*. Once tool in lesion was confirmed, biopsies were taken under similar breath-hold.

ENB was described previously (8). In summary, thin-sliced CT imaging was imported into the ENB software (iLogic 7.0, superDimension), in which virtual bronchoscopic images were reconstructed. Anatomic landmarks (right upper lobe, right lower lobe, main carina, left lower lobe, left upper lobe) were identified to complete radiologic mapping. Next, the preferred Edge extended working channel catheter (Medtronic, Inc., Dublin, Ireland) with 180 or 90 degrees was selected alongside the standard locatable guide to use in each case depending on nodule location. Regarding ssRAB, navigational planning was performed using PlanPoint (Intuitive Surgical, Sunnyvale, CA, USA) using a preprocedural CT scan of the chest. Next, the ssRAB was docked and robotic catheter with vision probe (Intuitive Surgical) inserted into the endotracheal tube. Registration was performed, followed by navigation to the target lesion(s).

Tissue samples were obtained using multimodality tools; Typically, fine needle for aspiration (Medtronic Arcpoint and Intuitive Surgical Flexision Ion) is performed first to confirm tool-in-lesion and to sample tissue. Next, biopsy forceps (Boston Scientific Radial Jaw; Marlborough, MA, USA) and cytology brush (Olympus Cytology brush) are used to acquire tissue. Targeted bronchoalveolar lavage is performed last. Furthermore, all patients underwent endobronchial ultrasound (EBUS)-guided transbronchial needle aspiration for mediastinal staging following navigational bronchoscopy. Rapid on-site pathologic examination was used for all cases. Tissue samples and cytology specimens were eventually evaluated by a dedicated lung pathologist.

Outcomes

The primary outcome was diagnostic yield for lung nodules between the two navigational platforms guided by CBCT. Two separate methods were used to calculate diagnostic yield as described previously (9). In the first method, diagnostic yield was defined as the presence of malignancy or benign histological findings (such as granuloma or infection) leading to a specific diagnosis at the time of bronchoscopy. Non-specific benign findings (inflammation, organizing pneumonia) are not considered true negatives in the first method. The second method includes the addition of longitudinal follow-up data for non-specific benign findings. These patients are followed and categorized as true negatives only if repeat biopsy or imaging is consistent with a nonmalignant diagnosis. Patients were followed for 12 months both clinically and radiographically. In cases where the patient did not have or lost follow up to document improvement in a non-malignant nodule, this was considered a false negative.

Navigational success was defined as needle tip within target lesion in three orthogonal plans for each separate lesion during CBCT imaging. Diagnostic accuracy was calculated as the rate of true-positives plus true-negatives divided by the total number of lung nodule biopsies performed after longitudinal follow-up. Sensitivity for malignancy was calculated as the true-positives divided by the true-positives and false-negatives after longitudinal follow-up. Procedural time was measured from the insertion of the bronchoscope to termination of the procedure.

Statistical analysis

Demographic and medical data were recorded. Continuous outcomes were presented as means or medians based on the assessment of normality (Shapiro-Wilk test). Parametric (*t*-test) and nonparametric (Wilcoxon rank-sum test) tests were applied to compare the data based on the normality assessment. Dichotomic outcomes were presented in proportions and were compared with the χ^2 test. A P value <0.05 was considered statistically significant. A stepwise multivariate regression model was performed based on the type of procedures including the following variables: target size, distance to the pleura, the number of CBCT spins performed, the number of nodules biopsied, the presence of bronchus sign, and diagnostic yield. Data were analyzed using STATA Release 14 (StataCore, College Station, TX, USA).

Results

Baseline patient and nodule characteristics

A total of 92 patients with 97 nodules underwent ENB-CBCT and 93 patients with 111 nodules underwent ssRAB-CBCT for pulmonary lesions. In the ENB-CBCT group, the median age was 68 years [interquartile range (IQR), 62–75 years], 54 (55.7%) were men, and 79 (81.4%) were active or former smokers. Patients in the ssRAB-CBCT group had a median age of 69 years (IQR, 64–74 years), 67 (60.4%) were men, and 90 (81.1%) were active or former smokers.

The median size of the nodule in the ENB-CBCT group was 16.5 mm (IQR, 12–22 mm) as compared with 12 mm (IQR, 9–16 mm) in the ssRAB-CBCT group (P<0.001). Regarding the average distance from the pleura, the ENB-CBCT group was 12 mm (IQR, 2.5–23 mm) from the pleura as compared with 8 mm (IQR, 2–19 mm) in the ssRAB-CBCT group (P=0.15). Nodule densities were similar between groups. The bronchus sign was present in 56 (57.7%) patients undergoing biopsy with ENB-CBCT as compared with 37 (33.3%) in the ssRAB-CBCT group (P<0.001). Most of the nodules were in the right upper lobe for the ENB-CBCT (26.8%) and for the ssRAB-CBCT group (30.6%). Baseline demographics and nodule characteristics are shown in *Table 1*.

Procedure characteristics

More patients in the ssRAB-CBCT group (31.5%) underwent biopsy of multiple nodules in a single procedure when compared to ENB-CBCT (10.3%) (P<0.001). The median total procedure time was similar in patients in the ENB-CBCT group as compared to the ssRAB-CBCT

Table 1 Clinical and nodule characteristics of the patients included in the study

Patients and nodules characteristics	ENB-CBCT (n=97)	ssRAB-CBCT (n=111)	P value
Age (years), median [IQR]	68 [62–75]	69 [64–74]	0.59
Men, n (%)	54 (55.7)	67 (60.4)	0.57
BMI (kg/m^2), median [IQR]	27.9 [21.8–32.0]	30.34 [25.9–34.2]	0.050
Former or current smoker, n (%)	79 (81.4)	90 (81.1)	0.55
Target size (mm), median [IQR]	16.5 [12–22]	12 [9–16]	<0.001
Distance from the pleura (mm), median [IQR]	12 [2.5–23]	8 [2–19]	0.15
Nodule density, n (%)			0.88
Solid	79 (81.4)	87 (78.4)	
Subsolid	12 (12.4)	18 (16.2)	
Ground glass	6 (6.2)	6 (5.4)	
Bronchus sign, n (%)	56 (57.7)	37 (33.3)	<0.001
Target location, n (%)			0.62
Right upper lobe	26 (26.8)	34 (30.6)	
Right middle lobe	10 (10.3)	8 (7.2)	
Right lower lobe	16 (16.5)	18 (16.2)	
Left upper lobe	25 (25.8)	35 (31.5)	
Left lower lobe	20 (20.6)	16 (14.4)	

ENB, electromagnetic navigation bronchoscopy; CBCT, cone-beam computed tomography; ssRAB, shape-sensing robotic assisted bronchoscopy; IQR, interquartile range; BMI, body mass index.

group (P=0.09). In the ENB-CBCT group, patients underwent an average of one CBCT spin as compared to an average of two CBCT spins in the ssRAB-CBCT group (P<0.001). When evaluating CBCT imaging, 70% of nodules in the ENB-CBCT group had tool in lesion within the nodule, while 83% of nodules in the ssRAB-CBCT group had tool in lesion within the nodule (P=0.03). In the ssRAB-CBCT group, five patients did not have repeat CBCT imaging to document tool in lesion due to positive diagnosis on rapid on-site evaluation (ROSE). The overall rate of adverse events was similar in both groups (P=0.77). Most common complication was pneumothorax, occurring in 2.1% and 1.8% of patients in the ENB-CBCT and ssRAB-CBCT groups, respectively. Procedural characteristics are shown in *Table 2*.

Diagnostic yield

Regarding the pathology results (*Table 3*), adenocarcinoma was the most common diagnosis in the ENB-CBCT group (42%) and in the ssRAB-CBCT group (56.3%). Among patients undergoing ENB-CBCT, 51.5% of lung nodules (50/97) were malignant and 14.4% of lung nodules (14/97) showed specific benign histopathologic features. Among patients undergoing ssRAB-CBCT, 64% of nodules (71/111) were malignant and 25.2% (28/111) showed specific benign histopathologic features. In the ENB-CBCT group, the sensitivity for malignancy was 79.37% as compared to 95.95% in the ssRAB-CBCT group (P=0.003). Diagnostic accuracy for ENB-CBCT was 86.60% as compared to 97.30% in the ssRAB-CBCT group (P=0.007). Prevalence of malignancy in ENB-CBCT group was 64.95%, while prevalence in the ssRAB-CBCT group was 66.67% (P=0.88) (*Table 4*).

The diagnostic yield at time of bronchoscopy (*Table 4*) in ENB-CBCT was 66% (64/97) as compared to 89% (99/111) in the ssRAB-CBCT (P<0.001). Regarding the diagnostic yield when including follow-up (*Table 4*), ENB-CBCT had a diagnostic yield of 79% (77/97) as compared to 94.6% (105/111) in ssRAB-CBCT (P=0.001). Following

Table 2 Procedural characteristics

Characteristics	ENB-CBCT (n=97)	ssRAB-CBCT (n=111)	P value
Number of nodules sampled, n [%]			<0.001
One	87 [89.7]	76 [68.5]	
Two	10 [10.3]	32 [28.8]	
Three	0	3 [2.7]	
Bronchoscopy time (min), median [IQR]	102 [84–133]	103 [82–119]	0.09
Fluoroscopy time (min), median [IQR]	9.75 [7.8–12.53]	15.1 [10.88–18.68]	<0.001
Target visible in fluoroscopy, n [%]	51 [52.6]	35 [31.5]	0.004
Tool in lesion on CBCT, n [%]†			0.03
Within	68 [70.1]	88 [83]	
Adjacent	29 [29.9]	18 [17]	
CBCT radiation dose (mSv), median [IQR]	3.53 [1.57–6.21]	2.97 [1.92–4.83]	0.12
CBCT spins, median [IQR]	1 [1–1]	2 [1–2]	<0.001
Linear EBUS sampling, n [%]	77 [79.4]	87 [78.4]	>0.99
Adverse events, n [%]	5 [5.2]	7 [6.3]	0.77
Pneumothorax	2 [2.1]	2 [1.8]	
Bleeding	0	2 [1.8]	
Hypoxic respiratory failure	1 [1]	1 [1]	
Hemodynamic instability	2 [2.1]	2 [1.8]	

†, in the ssRAB-CBCT group, five patients did not have repeat CBCT imaging to document tool in lesion. ENB, electromagnetic navigation bronchoscopy; CBCT, cone-beam computed tomography; ssRAB, shape-sensing robotic-assisted bronchoscopy; IQR, interquartile range; EBUS, endobronchial ultrasound.

multivariate regression analysis adjusting for the size of the lesion, distance from the pleura, the number of CBCT spins performed, the number of nodules biopsied, and presence of bronchus sign, the odds ratio for the diagnostic yield was 4.72 [95% confidence interval (CI): 2.05–10.85, P<0.001] in the ssRAB-CBCT group as compared with ENB-CBCT respectively.

Regarding the size of the nodules biopsied, the diagnostic yield at time of bronchoscopy in lesions ≤10 mm in size was 50% in the ENB-CBCT and 84% in the ssRAB-CBCT group respectively (P=0.01). Nodules between 11 and 20 mm had a diagnostic yield of 64% in the ENB-CBCT and 92.7% in the ssRAB-CBCT group (P<0.001). However, nodules between 21 and 30 mm had a diagnostic yield of 69.23% in the ENB-CBCT and 100% in the ssRAB-CBCT group (P=0.24).

Regarding the size of nodules biopsied, the diagnostic yield including follow-up in lesions ≤10 mm in size was 68.75% in the ENB-CBCT and 90.91% in the ssRAB-CBCT group (P=0.04). Lesions between 11 and 20 mm had a diagnostic yield of 79.25% in the ENB-CBCT and 96.4% in the ssRAB group (P=0.007). Lesions between 21 and 30 mm had a diagnostic yield of 76.92% in the ENB-CBCT and 100% in the ssRAB-CBCT group (P=0.52).

Discussion

This retrospective review of 185 patients with pulmonary nodules undergoing biopsy with ssRAB-CBCT as compared to ENB-CBCT showed a 23.2% and 15.2% absolute increase in diagnostic yield at time of bronchoscopy and when incorporating follow-up data, respectively. To the best of our knowledge, this is the first study comparing ENB and ssRAB using an advanced real time imaging technique in both groups and thus removing CT-to-body divergence as a confounding factor. CBCT allowed for real-time

Table 3 Final pathological diagnosis

Pathological diagnosis	ENB-CBCT (n=97)	ssRAB-CBCT (n=111)
Diagnostic pathology		
Malignant diagnoses, n [%]	50 [51.5]	71 [64]
Small cell lung cancer	3 [6]	1 [1.4]
Adenocarcinoma	21 [42]	40 [56.3]
Squamous cell	20 [40]	23 [32.4]
Other malignancy	6 [12]	7 [9.9]
Benign diagnoses, n [%]	14 [14.4]	28 [25.2]
Infection	9 [64.3]	9 [32.1]
Granuloma	2 [14.3]	14 [50]
Other specific benign	3 [21.4]	5 [17.9]
Non diagnostic pathology, n [%]	33 [34]	12 [10.8]
Inflammation	17 [51.5]	8 [66.7]
Normal/atypical tissue	16 [48.5]	4 [33.3]

ENB, electromagnetic navigation bronchoscopy; CBCT, cone-beam computed tomography; ssRAB, shape-sensing robotic-assisted bronchoscopy.

verification of biopsy tools, repositioning of the navigational catheter, if necessary, and highlighting the nodule while performing biopsies using enhanced fluoroscopy images (*Figure 2*). After performing a stepwise regression model adjusting for size of the target lesion, distance from the pleura, the presence of bronchus sign, the number of CBCT spins performed, and the number of nodules biopsied, we found an odds ratio for the diagnostic yield of 4.72 (95% CI: 2.05–10.85, P<0.001) in the ssRAB-CBCT as compared with the ENB-CBCT group, showing that the results were independent of such factors.

Several definitions for diagnostic yield have been proposed in the literature (9-11). We opted to use two definitions that are clinically useful and are mostly impactful in daily practice. The first method calculates histological findings that lead to a specific diagnosis at the time of bronchoscopy, however, this may underestimate diagnostic yield due to lack of longitudinal follow-up. The second method includes the addition of follow-up data for non-specific benign findings with subsequent surveillance imaging or biopsy. Patients with biopsy findings such as normal lung parenchyma, atypia, or benign bronchial cells

Table 4 Diagnostic yield and sensitivity for malignancy

Diagnostic outcomes	ENB-CBCT (n=97)	ssRAB-CBCT (n=111)	P value
Diagnostic yield at time of bronchoscopy, % (N/D)	66 (64/97)	89 (99/111)	<0.001
Diagnostic yield with longitudinal follow-up, % (N/D)	79 (77/97)	94.6 (105/111)	0.001
Sensitivity, % (N/D) [95% CI]	79.37 (50/63) [63.30–88.53]	95.95 (71/74) [88.61–99.16]	0.003
Diagnostic accuracy, % (N/D) [95% CI]	86.60 (84/97) [78.17–92.67]	97.30 (108/111) [92.30–99.44]	0.007
Prevalence, % (N/D) [95% CI]	64.95 (63/97) [54.59–74.36]	66.67 (74/111) [57.09–75.33]	0.88
Diagnostic yield by nodule size			
≤10 mm			
At time of bronchoscopy, % (N/D)	50 (8/16)	84.09 (37/44)	0.01
Longitudinal follow-up, % (N/D)	68.75 (11/16)	90.91 (40/44)	0.04
11–≤20 mm			
At time of bronchoscopy, % (N/D)	64.15 (34/53)	92.73 (51/55)	<0.001
Longitudinal follow-up, % (N/D)	79.25 (42/53)	96.4 (53/55)	0.007
21–≤30 mm			
At time of bronchoscopy, % (N/D)	69.23 (9/13)	100 (7/7)	0.24
Longitudinal follow-up, % (N/D)	76.92 (10/13)	100 (7/7)	0.52

ENB, electromagnetic navigation bronchoscopy; CBCT, cone-beam computed tomography; ssRAB, shape-sensing robotic-assisted bronchoscopy; N, numerator; D, denominator; CI, confidence interval.

were regarded as non-diagnostic.

This increase in diagnostic yield is likely secondary to the improved airway segmentation of ssRAB and small footprint of the robotic catheter, which allows the bronchoscopist to navigate deep into the periphery of the lung. Furthermore, the articulating robotic catheter can aid in biopsy success by allowing for small, accurate corrections in biopsy trajectory under CBCT guidance. Once the preferred catheter position is achieved, the robotic catheter has increased stability when compared to the ENB catheter, allowing for a more accurate biopsy, regardless of tool used. Our ssRAB-CBCT diagnostic yield is comparable to other publications, ranging from 77% to 94% (12-14), as was our ENB-CBCT diagnostic yield (8,15,16). Prevalence of malignancy can also affect diagnostic yield (10). When comparing the ENT-CBCT and ssRAB-CBCT groups, the prevalence of malignancy was similar (P=0.88) and our overall prevalence of malignancy was 65.86%, which is comparable to other studies (58–64.1%) (17,18) and may decrease the chance of prevalence of malignancy being a confounder in the calculation of diagnostic yield.

Our navigational success as defined by tool within lesion for ENB-CBCT was lower as compared to ssRAB-CBCT group, which may contribute to our increased diagnostic yield in the ssRAB-CBCT group. However, dedicated studies investigating the relationship between tool in lesion and diagnostic yield are warranted to confirm. The number of times we used CBCT spins was less in the ENB-CBCT group. This is likely due to the need to achieve tool in lesion confirmation for smaller, more challenging nodules in the ssRAB-CBCT group, requiring additional spins. Additionally, we biopsied multiple nodules more frequently in the ssRAB-CBCT group (31.5% *vs.* 10.3%), necessitating additional confirmatory CBCT spins. Overall procedure time was similar, despite a significantly smaller average nodule size as well as a higher percentage of cases having multiple target lesions in the ssRAB-CBCT group.

Our study has limitations that are inherent to a retrospective study. First, our study cohorts were investigated sequentially, which may introduce a bias as the learning curve for navigational bronchoscopy and CBCT may affect diagnostic success. However, both bronchoscopists had significant navigational and CBCT experience prior to the acquisition of this data. Additionally, the acquired data was the last 92 cases of EMN-CBCT and the first 93 cases of ssRAB-CBCT at our institution. Thus, we feel the learning curve for EMN-CBCT is less impactful to the lower diagnostic yield in these patients. Additionally, the accessibility to such a hybrid room and the cost related to the combined use of CBCT and navigational platforms could limit the overall generalizability of our study in some centers. However, utilization of advanced imaging [C-arm based tomosynthesis (illumisite), mobile CBCT (mobile 3D C-arm Machine Cios Spin) and O-arm CT] along with available navigational platforms to counteract CT-to-body divergence is increasing (19).

Higher ionizing radiation exposure compared to X-ray fluoroscopy could represent a potentially important disadvantage of CBCT guidance over traditional fluoroscopy. Our study showed median radiation exposure under CBCT guidance of 3.53 and 2.97 mSv in ENB and ssRAB groups, respectively, which is generally higher than the exposure reported for biopsy performed under X-ray fluoroscopy (0.49 mSv) (20). However, this is comparable to the exposure reported in similar studies using navigational platforms under CBCT guidance and average radiation exposure from CT-guided diagnostic and therapeutic procedures of chest and abdomen (16,21-25).

Conclusions

The use of intraprocedural CBCT for real-time confirmation in conjunction with ssRAB has shown to significantly increase diagnostic yield for pulmonary nodules as compared to ENB, specifically for nodules of ≤20 mm. The above findings need to be confirmed in multicenter prospective trials.

Acknowledgments

A portion of this data was presented at the 2023 AABIP meeting in Chicago, IL, USA.
Funding: None.

Footnote

Reporting Checklist: The authors have completed the STROBE reporting checklist. Available at https://jtd.amegroups.com/article/view/10.21037/jtd-24-178/rc

Data Sharing Statement: Available at https://jtd.amegroups.com/article/view/10.21037/jtd-24-178/dss

Peer Review File: Available at https://jtd.amegroups.com/article/view/10.21037/jtd-24-178/prf

Conflicts of Interest: All authors have completed the ICMJE

uniform disclosure form (available at https://jtd.amegroups.com/article/view/10.21037/jtd-24-178/coif). F.K. serves as an unpaid Associate Editor-in-Chief of *Journal of Thoracic Disease* from May 2024 to April 2026. R.A. received nonemployee compensation (consultant) from Intuitive Surgical Inc. for providing education and case proctoring, and speakers bureaus from Intuitive Surgical Inc. for giving educational lectures. D.B. received nonemployee compensation (consultant) from Intuitive Surgical Inc. for providing education and case proctoring to new physician users of robotic bronchoscopy so that new users could be credentialed in robotic bronchoscopy. The other authors have no conflicts of interest to declare.

Ethical Statement: The authors are accountable for all aspects of the work in ensuring that questions related to the accuracy or integrity of any part of the work are appropriately investigated and resolved. The study was conducted in accordance with the Declaration of Helsinki (as revised in 2013). This study was approved by Tulane University School of Medicine Institutional Review Board (No. 2023-128) and informed consent for this retrospective analysis was waived.

References

1. Gould MK, Tang T, Liu IL, et al. Recent Trends in the Identification of Incidental Pulmonary Nodules. Am J Respir Crit Care Med 2015;192:1208-14.
2. Goldstraw P, Chansky K, Crowley J, et al. The IASLC Lung Cancer Staging Project: Proposals for Revision of the TNM Stage Groupings in the Forthcoming (Eighth) Edition of the TNM Classification for Lung Cancer. J Thorac Oncol 2016;11:39-51.
3. Tanner NT, Yarmus L, Chen A, et al. Standard Bronchoscopy With Fluoroscopy vs Thin Bronchoscopy and Radial Endobronchial Ultrasound for Biopsy of Pulmonary Lesions: A Multicenter, Prospective, Randomized Trial. Chest 2018;154:1035-43.
4. Kops SEP, Heus P, Korevaar DA, et al. Diagnostic yield and safety of navigation bronchoscopy: A systematic review and meta-analysis. Lung Cancer 2023;180:107196.
5. Kalchiem-Dekel O, Connolly JG, Lin IH, et al. Shape-Sensing Robotic-Assisted Bronchoscopy in the Diagnosis of Pulmonary Parenchymal Lesions. Chest 2022;161:572-82.
6. Simoff MJ, Pritchett MA, Reisenauer JS, et al. Shape-sensing robotic-assisted bronchoscopy for pulmonary nodules: initial multicenter experience using the Ion™ Endoluminal System. BMC Pulm Med 2021;21:322.
7. Yu Lee-Mateus A, Reisenauer J, Garcia-Saucedo JC, et al. Robotic-assisted bronchoscopy versus CT-guided transthoracic biopsy for diagnosis of pulmonary nodules. Respirology 2023;28:66-73.
8. Kheir F, Thakore SR, Uribe Becerra JP, et al. Cone-Beam Computed Tomography-Guided Electromagnetic Navigation for Peripheral Lung Nodules. Respiration 2021;100:44-51.
9. Vachani A, Maldonado F, Laxmanan B, et al. The Impact of Alternative Approaches to Diagnostic Yield Calculation in Studies of Bronchoscopy. Chest 2022;161:1426-8.
10. Vachani A, Maldonado F, Laxmanan B, et al. The Effect of Definitions and Cancer Prevalence on Diagnostic Yield Estimates of Bronchoscopy: A Simulation-based Analysis. Ann Am Thorac Soc 2023;20:1491-8.
11. Leonard KM, Low SW, Echanique CS, et al. Diagnostic Yield vs Diagnostic Accuracy for Peripheral Lung Biopsy Evaluation: Evidence Supporting a Future Pragmatic End Point. Chest 2024;165:1555-62.
12. Chambers J, Knox D, Leclair T. O-arm CT for Confirmation of Successful Navigation During Robotic Assisted Bronchoscopy. J Bronchology Interv Pulmonol 2023;30:155-62.
13. Vu LH, Yu Lee-Mateus A, Edell ES, et al. Accuracy of Preliminary Pathology for Robotic Bronchoscopic Biopsy. Ann Thorac Surg 2023;116:1028-34.
14. Benn BS, Romero AO, Lum M, et al. Robotic-Assisted Navigation Bronchoscopy as a Paradigm Shift in Peripheral Lung Access. Lung 2021;199:177-86.
15. Bondue B, Taton O, Tannouri F, et al. High diagnostic yield of electromagnetic navigation bronchoscopy performed under cone beam CT guidance: results of a randomized Belgian monocentric study. BMC Pulm Med 2023;23:185.
16. Pritchett MA, Schampaert S, de Groot JAH, et al. Cone-Beam CT With Augmented Fluoroscopy Combined With Electromagnetic Navigation Bronchoscopy for Biopsy

of Pulmonary Nodules. J Bronchology Interv Pulmonol 2018;25:274-82.
17. Styrvoky K, Schwalk A, Pham D, et al. Shape-Sensing Robotic-Assisted Bronchoscopy with Concurrent use of Radial Endobronchial Ultrasound and Cone Beam Computed Tomography in the Evaluation of Pulmonary Lesions. Lung 2022;200:755-61.
18. Khan F, Seaman J, Hunter TD, et al. Diagnostic outcomes of robotic-assisted bronchoscopy for pulmonary lesions in a real-world multicenter community setting. BMC Pulm Med 2023;23:161.
19. Ravikumar N, Ho E, Wagh A, et al. Advanced Imaging for Robotic Bronchoscopy: A Review. Diagnostics (Basel) 2023;13:990.
20. Steinfort DP, Einsiedel P, Irving LB. Radiation dose to patients and clinicians during fluoroscopically-guided biopsy of peripheral pulmonary lesions. Respir Care 2010;55:1469-74.
21. Verhoeven RLJ, van der Sterren W, Kong W, et al. Cone-beam CT and Augmented Fluoroscopy-guided Navigation Bronchoscopy: Radiation Exposure and Diagnostic Accuracy Learning Curves. J Bronchology Interv Pulmonol 2021;28:262-71.
22. Casal RF, Sarkiss M, Jones AK, et al. Cone beam computed tomography-guided thin/ultrathin bronchoscopy for diagnosis of peripheral lung nodules: a prospective pilot study. J Thorac Dis 2018;10:6950-9.
23. Hohenforst-Schmidt W, Zarogoulidis P, Vogl T, et al. Cone Beam Computertomography (CBCT) in Interventional Chest Medicine - High Feasibility for Endobronchial Realtime Navigation. J Cancer 2014;5:231-41.
24. Mettler FA Jr, Huda W, Yoshizumi TT, et al. Effective doses in radiology and diagnostic nuclear medicine: a catalog. Radiology 2008;248:254-63.
25. Guberina N, Forsting M, Ringelstein A, et al. Radiation exposure during CT-guided biopsies: recent CT machines provide markedly lower doses. Eur Radiol 2018;28:3929-35.

Cite this article as: Abdelghani R, Espinoza D, Uribe JP, Becnel D, Herr R, Villalobos R, Kheir F. Cone-beam computed tomography-guided shape-sensing robotic bronchoscopy *vs.* electromagnetic navigation bronchoscopy for pulmonary nodules. J Thorac Dis 2024;16(9):5529-5538. doi: 10.21037/jtd-24-178